JOURNAL OF CATALYSIS **161,** 829–838 (1996)
ARTICLE NO. 0246

Magnesium Oxides as Basic Catalysts for Organic Processes

Study of the Dehydrogenation–Dehydration of 2-Propanol

M. A. Aramendía,[1] V. Borau, C. Jiménez, J. M. Marinas, A. Porras, and F. J. Urbano

Departamento de Química Orgánica, Facultad de Ciencias, Universidad de Córdoba, Avenida San Alberto Magno s/n, E-14004 Córdoba, Spain

Received June 7, 1995; revised March 6, 1996; accepted March 22, 1996

The reactivity of various magnesium oxides in the gas-phase dehydrogenation–dehydration of 2-propanol was studied by using a tubular flow reactor. The oxides were synthesized from different precursors by using various methods. The influence of the precursor used, *in vacuo* calcination and B_2O_3 doping was analyzed in the light of the results obtained in the above-mentioned test reaction. Potential correlations between the surface acid–base properties of the oxides and the kinetic constants of dehydrogenation and dehydration obtained for the test reaction were sought. Also, potential sources of deactivation for the catalysts were investigated. Carbon deposits observed by temperature-programmed oxidation and the presence of strongly adsorbed species following an isothermal reaction, which were detected by temperature-programmed desorption, were found to be the two primary sources. Finally, the reaction mechanism was studied; the two proposed pathways are consistent with the results obtained.

INTRODUCTION

The acid strength of catalysts can be measured by using a variety of test reactions (1–7). However, procedures for measuring the basic strength of catalytic solids are relatively few (8). The transformation of 2-propanol is a widely used test reaction for characterizing both the acidic and basic properties of solids (9). Reported applications involve the use of a variety of oxides of such elements as zirconium (10, 11), magnesium (12), calcium (12, 13), barium (12), zinc, titanium, and vanadium (11), and aluminum (14), among others. On contact with an acidic or basic solid, 2-propanol undergoes three types of competitive reactions, namely: (a) intramolecular dehydration, which yields propene and water; (b) intermolecular dehydration, which gives diisopropyl ether; and (c) dehydrogenation to acetone and hydrogen.

While the surface acid–base properties of the solids are known to be responsible for the three above-mentioned reaction types, the specific role of each property in each process remains obscure. Thus, the initial rates of dehydration and dehydrogenation have been correlated by many authors with the acidity and basicity, respectively, of the solid used (15); others, however, have found interesting correlations between the ratio of both initial rates and the overall basicity of the catalyst employed (16, 17). Activation parameters such as the Arrhenius activation energy for the dehydration and dehydrogenation process allow one to characterize surface sites in terms of nature, strength, size, etc. (17), which can be of great assistance in elucidating reaction mechanisms.

Programmed temperature techniques have become major tools for investigating some processes. Thus, Waugh *et al*. (18) used temperature-programmed surface reaction (TPSR) experiments to elucidate the kinetics and mechanism of 2-propanol decomposition over various metal oxides. Similarly, various surface properties of solids have been determined from temperature-programmed desorption (TPD) experiments involving probe molecules preadsorbed on a catalyst (8, 19, 20).

In this work we used the dehydration–dehydrogenation of 2-propanol as a model reaction to characterize various magnesium oxides. Isothermal gas-phase reactions were used to derive kinetic data for the reaction over the temperature range 200–500°C. In addition, temperature-programmed surface reaction (TPSR), oxidation (TPO), and desorption (TPD) experiments were carried out in order to obtain information about surface adsorption, reaction, and deactivation phenomena involved in the decomposition of 2-propanol over basic MgO catalysts. Finally, potential correlations between the *pseudo*-kinetic constants for the different processes and the acidity and basicity of the solids, derived from temperature-programmed desorption experiments (TPD–MS) with probe compounds such as pyridine, 2,6-dimethyl-pyridine, and CO_2 were sought. For comparison, the results for a typical acid catalyst (PM2), that was previously thoroughly characterized by our group, are also reported.

[1] To whom all correspondence should be addressed.

0021-9517/96 $18.00

EXPERIMENTAL

Catalyst Synthesis

The magnesium oxides used were prepared from two different precursors, namely: (a) $Mg_5(OH)_2(CO_3)_4 \cdot 4H_2O$ (Merck Art. 5827), which produced the catalysts named MgO(I)AIR and MgO(I)VAC; and (b) $Mg(OH)_2$ (Merck Art. 5870), which provided the solid named MgO(II)AIR. All tested solids were obtained by calcination in a ceramic crucible, either in the air or *in vacuo* (hence AIR and VAC, respectively, at the end of the catalyst names) by heating from room temperature to 600°C at a rate of 4°C/min and then keeping the final temperature for 2 h, after which the solids were allowed to cool back to room temperature.

The catalyst designated BM50 was prepared by suspending 29.0 g of $Mg(OH)_2$ and 0.35 g of B_2O_3 in 200 mL of distilled water and sonicating the mixture for 1 h. The resulting solid was dried in a stove at 120°C for 2 h and calcined by using the above-described temperature programme. The Mg/B ratio thus obtained was 50 : 1.

Catalyst PM2 was synthesized from silica gel, $AlCl_3 \cdot 6H_2O$, and H_3PO_4 (85% by weight). The final composition of the solid was 20 : 80 w/w $AlPO_3/SiO_2$. The synthetic procedure for this catalyst is described in detail elsewhere (21).

Acid–Base and Textural Properties

Table 1 summarizes the textural and acid–base properties of the catalysts. Textural properties were determined by means of a Micromeritics ASAP 2000 poremeter, while acid–base properties were assessed by temperature-programmed desorption-mass spectrometry (TPD–MS) of probe molecules using a procedure described in a previous paper (19, 20). The probe molecules used were pyridine (PY) for total acidity, 2,6-dimethylpyridine (DMPY) for Brønsted acidity, and CO_2 for total basicity. This method allows us to obtain the number of acid and basic sites, as well as their relative strengths related to the desorption temperature of the probe molecule.

Continuous-Flow Isothermal Reactions

The quartz reactor used was 20 cm long × 1 cm i.d. and withstood temperatures of up to 1000°C. It was accommodated inside a furnace furnished with a device for adjusting the temperature to within ±1°C. The reactor outlet was connected on-line to a VG Sensorlab mass spectrometer from Fisons Instruments, plc/VG quadrupoles (East Sussex, UK) which was operated in the multiple ion monitoring (MIM) mode. The monitored peaks and the relative abundances for each compound, obtained from the Eight Peak Index of Mass Spectra (The Royal Society of Chemistry, Nottingham, UK), are given in Table 2.

TABLE 2

Monitored Peaks in the Mass Spectrometer (*m/z*) and Relative Abundances (RA) for the Different Compounds Studied

Compound	*m/z*	RA
2-Propanol	45	100
Acetone	58	33
Propene	41	100
Water	18	100
Hydrogen	2	100
Carbon dioxide	44	100
Diisopropyl ether	87	100

A fresh catalytic bed was used in each isothermal reaction and a nitrogen stream flowing at a rate of 120 mL/min was used as the carrier gas; 2-Propanol (Aldrich Art. 17,598-7) was injected at a controlled rate of 12 mL/h by means of a Braun perfuser. The catalyst weight used was 50 mg, the temperature stabilization time 20 min, and the reaction time 150 min in every case. The absence of internal and external diffusion under the reaction conditions used was checked before each experiment.

Programmed Temperature Tests

After each isothermal reaction, the catalyst was subjected to TPD or TPO in order to detect any molecular species that might have been strongly adsorbed on the catalyst or the amount of carbon deposit formed on its surface.

TPD experiments for adsorbed species on the catalyst surface were carried out according to the following protocol:

(a) Immediately after the isothermal reaction was finished, the reactor was rapidly cooled to room temperature by passing a nitrogen stream at 50 mL/min.

TABLE 1

Textural and Acid–Base Properties of the Magnesium Oxides Studied

Catalyst	S_{BET} $m^2 \cdot g^{-1}$	*Db* CO_2 $\mu mol \cdot m^{-2}$	Da_{Total} PY $\mu mol \cdot m^{-2}$	$Da_{Brønsted}$ DMPY $\mu mol \cdot m^{-2}$	Da_{Lewis} PY-DMPY $\mu mol \cdot m^{-2}$
MgO(II)AIR	119	4.252	0.294	0.252	0.042
BM50	104	4.231	0.346	0.269	0.077
MgO(I)VAC	69	6.319	0.449	0.391	0.058
MgO(I)AIR	60	3.334	0.483	0.417	0.067

Note. Db, basic site density; Da_{Total}, total acid site density; $Da_{Brønsted}$, Brønsted acid site density; Da_{Lewis}, Lewis acid site density.

(b) The reactor was then kept at room temperature while passing the nitrogen stream at the same flow-rate for at least 4 h in order to sweep any physisorbed species.

(c) Finally, the temperature was raised linearly from ambient to 600°C at 10°C/min under the nitrogen stream (50 mL/min).

The whole process was monitored via the mass spectrometer.

TPO experiments were also carried out after each isothermal reaction using the same procedure as with TPD tests, except that a stream consisting of 10% O_2/Ar was passed at 50 mL/min during application of the temperature ramp.

TPRS were carried out by bubbling nitrogen at 50 mL/min over propanol at 20°C and passing the alcohol-saturated gas over a fresh catalytic bed containing 50 mg of catalyst inside a tubular reactor. The temperature programme used comprised the following two stages:

(a) An isothermal stage at 100°C which lasted 30 min (until the 2-propanol flow and the MS signal stabilized).

(b) A heating ramp from 100 to 700°C at a rate of 10°C/min. The signals obtained and the reactants and products potentially responsible for them were monitored via the mass spectrometer.

RESULTS AND DISCUSSION

Temperature-Programmed Reactions

In order to obtain preliminary information about the influence of temperature on the different processes involved in the transformation of 2-propanol, we subjected it to temperature-programmed reactions over the four magnesium oxides and the acid catalyst (PM2). Figures 1 show the TPSR recordings obtained for solids MgO(II)AIR (Fig. 1A) and PM2 (Fig. 1B). The differential behavior of the signals for acetone and propene over both catalysts is quite interesting and reflects the differences in their acid–base properties. Graphs similar to that of Fig. 1A were obtained for the other magnesium oxides, even though over different temperature ranges and of different slopes for the monitored signals. In the light of these results, isothermal reactions were carried out over the temperature range 200–500°C.

Isothermal Reactions in a Flow-Through Reactor

Table 3 shows the conversions to acetone (dehydrogenation) and propene (dehydration), respectively, obtained with all the catalysts tested after a reaction time of 60 min (i.e., once the steady state had been reached). The amount of di-isopropyl ether obtained was negligible in every case, so it is not reported.

Catalysts MgO(II)AIR, BM50 and MgO(I)VAC exhibit virtually the same dehydrogenating activity, especially below 400°C. Above 400°C, MgO(I)VAC is slightly less active than the other two, which perform similarly in this respect.

Table 3 also reveals the effect of *in vacuo* calcination. Thus, catalyst MgO(I)AIR has a very low dehydrogenating activity relative to MgO(I)VAC. In terms of surface chemical properties (summarized in Table 1), the primary difference between these solids lies in the density and strength of

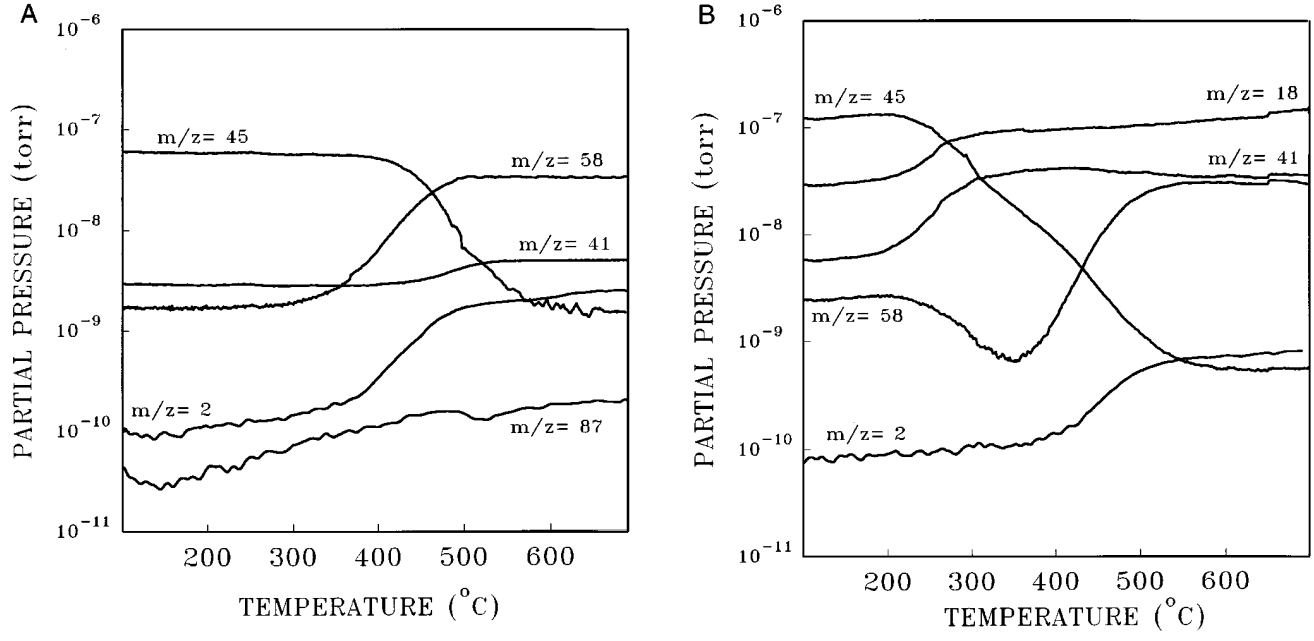

FIG. 1. Temperature-programmed surface reaction (TPSR) profiles for the catalysts MgO(II)AIR (A) and PM2 (B). Reaction conditions: Nitrogen flow, 50 mL/min; temperature rate, 10°C/min; catalyst weight, 50 mg ($m/z = 45$ (2-propanol), 58 (acetone), 41 (propene), 2 (hydrogen), 87 (di-isopropyl ether), 18 (water)).

TABLE 3

Percent Conversion to Acetone (X_a) and Propene (X_p) in the Decomposition of 2-Propanol

	Temperature (°C)													
	200		250		300		350		400		450		500	
Catalyst	X_a	X_p	X_a	X_p	X_a	X_p	X_a	X_p	X_a	X_p	X_a	X_p	X_a	X_p
MgO(II)AIR	9.5	10.8	11.3	12.2	13.9	13.4	15.5	11.7	21.4	10.1	28.5	9.4	36.7	8.6
BM50	9.9	12.1	10.4	12.3	11.3	12.4	13.6	13.3	18.9	12.3	27.4	12.2	35.9	10.4
MgO(I)VAC	9.2	10.7	11.0	11.4	12.7	11.3	15.5	10.8	20.4	8.7	24.4	7.7	31.0	7.1
MgO(I)AIR	5.3	5.9	5.7	5.8	6.4	6.2	7.7	6.3	12.3	7.2	17.5	6.6	22.1	5.9
PM2	1.5	19.9	1.2	29.9	1.0	41.0	0.6	50.6	3.4	61.8	4.7	67.5	5.9	76.9

Note. Reaction conditions: catalyst weight 50 mg; reaction time 60 min; 2-propanol flow: 12 mL/h; Nitrogen flow: 120 mL/min.

their basic sites, which are much higher (almost twice) for the vacuum-calcined solid than for its air-calcined counterpart. On the other hand, the density of acid sites is virtually identical for both solids. It therefore seems that the better performance of the vacuum-calcined solid, MgO(I)VAC, in the dehydrogenation reaction can be ascribed to its higher surface basicity relative to the air-calcined solid.

Also, a comparison of the results for MgO(I)AIR and MgO(II)AIR reveals the influence of the synthetic precursor on equal calcination procedures. Thus, the solid made from magnesium hydroxide, MgO(II)AIR, exhibited a higher dehydrogenating power, which again is consistent with its higher surface basicity relative to MgO(I)AIR (Table 1); in addition to the different density of basic sites for the two catalysts, the fact that they were synthesized from different precursors may also have led to the formation of basic sites of different strengths. In fact, in TPD–MS of CO_2 profiles, we reported the presence of very strong basic sites in the solids prepared from $Mg(OH)_2$ that were absent from MgO(I)AIR. It therefore seems logical to assume that the difference in the behavior of these two solids towards 2-propanol must be due to both factors, viz. site density and site strength.

Activity in the dehydration of 2-propanol was lower than that in its dehydrogenation for all the solids studied, especially above 300°C (Table 3).

The effect of the addition of B_2O_3 over the magnesium oxide is apparent from a comparison of the dehydration results obtained for catalysts MgO(II)AIR and BM50, the sole difference between which was the presence of a small amount of B_2O_3 (Mg/B = 50/1) in the latter. The boron oxide may have joined the crystal structure of the solid or deposited on its surface. In ^{27}Al-NMR experiments on Al_2O_3-doped MgO, McKenzie *et al.* (22) found Al^{3+} to initially be a part of the oxide lattice and subsequently to concentrate on the catalyst surface as a result of calcination. They suggested that surface aluminum lay in a tetrahedral coordinated oxidic environment that disfavored acid-catalysed reactions such as the dehydration of 2-propanol. In our case, as the likely result of the synthetic procedure employed, doping MgO with B_2O_3 gave a catalyst (BM50) with a higher dehydrating power (about 15%) than its undoped counterpart, MgO(II)AIR; this suggests that the B_2O_3 environment allows its intrinsically acid properties to boost the dehydrating activity of the catalyst. The oxide is therefore highly likely to be present as a deposit on the catalyst surface. Thus, as can be seen from Table 1, BM50 exhibited a higher acid site density (about 17%) than MgO(II)AIR but an essentially similar nature and strength in its sites (19, 20).

Finally, the acid catalyst (PM2), while providing a higher overall conversion, led to much less dehydrogenation and much more dehydration (consistent with its essentially acidic nature (21)) than the four magnesium oxides.

Influence of Temperature on the Selectivity

The selectivity towards acetone (S_a) and propene (S_p) was calculated from the following expressions:

$$S_a = \frac{\%\text{conv. acetone}}{\%\text{total conv.}} \times 100 \quad [1]$$

$$S_p = 100 - S_a. \quad [2]$$

Changes in S_a and S_p with temperature were of particular interest. Figure 2 shows the variation of S_a with this parameter at a reaction time of 60 min. As can be seen, catalyst PM2 behaved rather differently from the rest. Thus, while the latter exhibited a high selectivity towards the dehydrogenation product, the former gave propene preferentially. Also, S_a increased and then S_p decreased with the increase in the temperature for all the magnesium oxide catalysts. In searching for an explanation for these trends, one should bear in mind that the dehydration is widely accepted to take place via acid sites and the dehydrogenation through basic sites. As shown in previous works (19, 20), the ratio of acid to basic sites in the solids changed with temperature. Thus, those sites acting as acids against pyridine virtually disappeared above 250°C (except for very strong Lewis acid sites in the vacuum-calcined catalyst, MgO(I)VAC, which

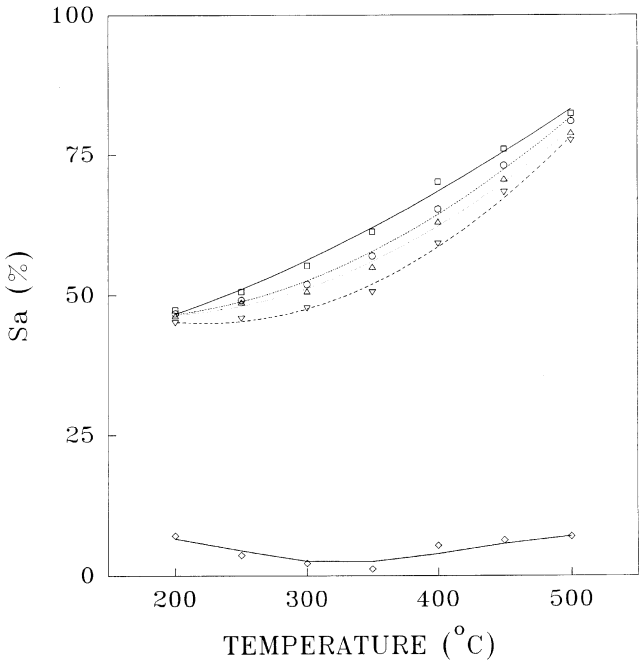

FIG. 2. Variation of the selectivity towards acetone (S_a) as a function of the reaction temperature for the different catalysts studied. Reaction time 60 min: (○), MgO(II)AIR; (□), MgO(I)VAC; (△), MgO(I)AIR; (▽), BM50; (◇), PM2.

disappeared at about 400°C). On the other hand, basic sites against CO_2 remained active above 400°C in all catalysts (and even above 600°C in the solids prepared from magnesium hydroxide). In fact, the number of basic sites (i.e., those effecting the dehydrogenation) increased, whereas that of acid sites (i.e., those responsible for the dehydration) decreased with increasing temperature, which resulted in an increase in S_n and a decrease in S_p, respectively.

Kinetic Study of the Dehydration–Dehydrogenation of 2-Propanol

Both the dehydrogenation and the dehydration of the alcohol were found to follow a first-order kinetics described by the Basset–Habgood equation [3],

$$\ln\left(\frac{1}{1-x}\right) = kK\frac{W}{F}RT, \qquad [3]$$

where k is the kinetic constant, K is the constant of adsorption of the catalyst surface, W is the catalyst weight, F is the reactant flow-rate, and x is the conversion. Using the initial-rate method (23, Eq. [3]) allowed us to obtain the product kK (the *pseudo*-kinetic constant) at each temperature tested for both processes (dehydration and dehydrogenation). Their activation energies were derived from the Arrhenius equation

$$k = A\exp\left(-\frac{E_a}{RT}\right), \qquad [4]$$

where k is the kinetic constant, A is the preexponential factor, R is the gas constant, T is temperature, and E_a is the activation energy.

The results obtained for the two competitive processes are given in Table 4. As can be seen, every magnesium oxide exhibited a similar E_a value in the dehydration and dehydrogenation.

The lower E_a values for the dehydration with PM2 relative to the magnesium oxides suggest that the former possesses more active dehydration sites than the latter. The E_a results for the dehydrogenation exhibit the opposite trend, so the oxides must have more active sites of this type than has catalyst PM2.

Correlation of Acidity and Basicity with Pseudo-Kinetic Constants

The widely documented correlation between the kinetic constant of dehydration for 2-propanol and the number of acid sites in the catalytic solid used is not so clear for the alcohol dehydrogenation. Some authors have correlated the number of basic sites with kinetic constants of dehydrogenation (15) and others with the ratio between both kinetic constants (dehydrogenation/dehydration). In this respect, Ai (24) claims that the dehydration of 2-propanol takes

TABLE 4

Preexponential Factors (ln A) and Activation Energies (E_a) Obtained from the Arrhenius Equation for the Dehydration and Dehydrogenation of 2-Propanol

	Dehydrogenation		Dehydration	
Catalyst	E_a (kJ mol^{-1})	ln A	E_a (kJ mol^{-1})	ln A
MgO(II)AIR	18.56 ± 1.15	−4.91 ± 0.34	17.43 ± 1.78	−9.15 ± 0.47
BM50	22.50 ± 1.35	−5.01 ± 0.53	14.08 ± 2.26	−8.49 ± 0.34
MgO(I)VAC	17.95 ± 2.02	−4.89 ± 0.25	15.56 ± 1.41	−8.73 ± 0.39
MgO(I)AIR	27.36 ± 1.70	−5.21 ± 0.63	23.93 ± 0.43	−9.72 ± 0.54
PM2	52.34 ± 2.61	−9.37 ± 0.95	10.52 ± 0.48	−7.97 ± 0.21

TABLE 5

Average *Pseudo*-Kinetic Constants of Dehydration (kK_p) and Dehydrogenation (kK_a) for 2-Propanol over the Catalysts Studied as Calculated by Using the Initial-Rate Method

Catalyst	$kK_a \times 10^5$	$kK_p \times 10^5$	kK_a/kK_p
MgO(II)AIR	310	65	4.769
BM50	337	68	4.956
MgO(I)VAC	598	83	7.205
MgO(I)AIR	295	90	3.278
PM2	45	516	0.087

place exclusively at acid sites, whereas its dehydrogenation involves both acid and basic sites.

In this work we investigated potential correlations between the average kinetic constants listed in Table 5 and the total acid site (Da_{tot}), the Brønsted acid site ($Da_{Brønsted}$), and the total basic site density (Db). The results are gathered in Table 6, together with their correlation coefficients and Student's t values at a 95% confidence level. As expected, the dehydrating activity was appreciably correlated with Brønsted and total acidity. Also, correlation between the kK_a/kK_p ratio and the basic site density was higher than that between kK_a and this density. These correlations are later justified on the basis of plausible reaction mechanisms.

Catalytic Deactivation

The isothermal reactions conducted at temperatures in the range 200–500°C gave decay profiles similar to those shown in Fig. 3 for MgO(I)VAC. All the reactions exhibited an initial period (not shown in the graphs) that lasted about 20 min, during which the reagent flow was unstable. After that, the conversion decreased and then levelled off at 50–60 min. During this period, each catalyst was deactivated to a different extent which increased with the increase in temperature. One potential origin for the deactivation was the carbon deposit formed on the catalyst surface. In this respect, the TPO tests performed after each reaction revealed the release of large amounts of CO_2 through the burning of deposited carbon on passing an O_2/Ar stream (25). Figure 4

TABLE 6

Correlations Between the Average *Pseudo*-Kinetic Constants of Dehydrogenation (kK_a) and Dehydration (kK_p) and the Basic Site Density (Db), Total Acid Site Density (Da_{Total}) and Brønsted Acid Site Density ($Da_{Brønsted}$)

Y	X	a	b	r	t-Student
$kK_a \cdot 10^5$	Db	−110	109	0.965	1.128
kK_a/kK_p	Db	−0.69	1.26	0.990	−1.137
$kK_p \cdot 10^5$	Da_{Total}	23.83	133.94	0.987	3.857
$kK_p \cdot 10^5$	$Da_{Brønsted}$	29.35	141.85	0.993	7.196

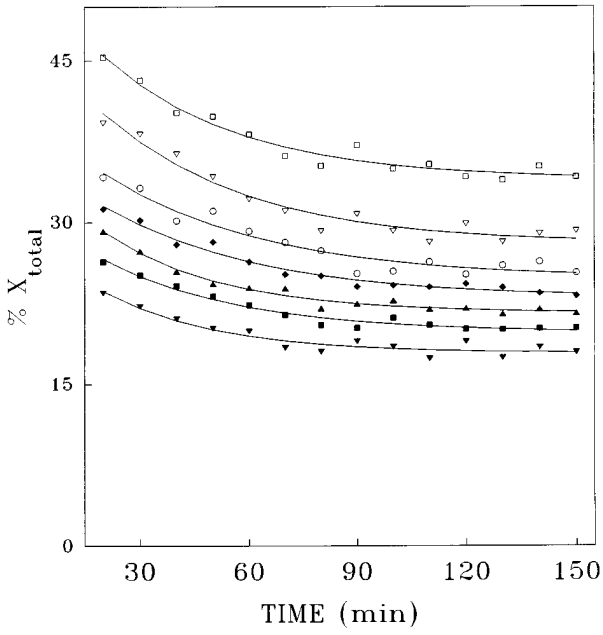

FIG. 3. Deactivation profiles (total conversion, X_{tot}, against time) for catalyst MgO(I)VAC at reaction temperatures from 200 to 500°C. Reaction conditions: catalyst weight, 50 mg; 2-propanol flow, 12 mL/h; nitrogen flow, 120 mL/min: (▼), 200°C, (■), 250°C; (▲), 300°C; (◆), 350°C; (◯), 400°C; (▽), 450°C; (□), 500°C.

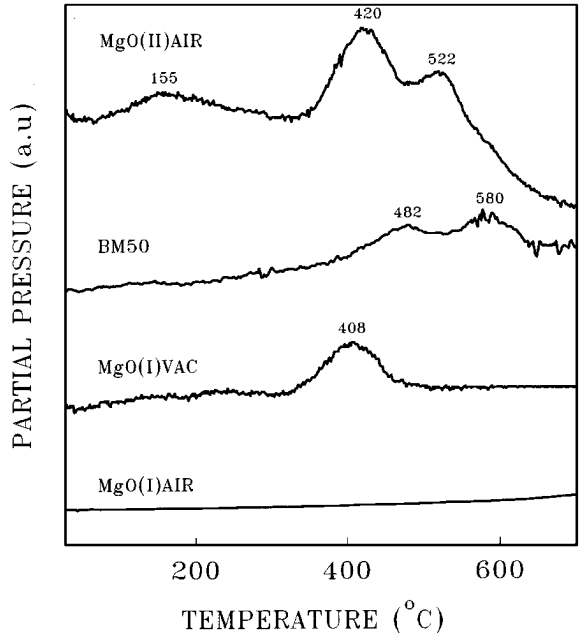

FIG. 4. TPO profiles for the magnesium oxides recorded following isothermal reactions at 200°C. Conditions: Flow of 10% O_2/Ar, 50 mL/min; temperature ramp, 10°C/min; catalyst weight, 50 mg. Peak monitored, $m/z = 44$.

TABLE 7

Area and Maximum Temperature (T_{max}) of the CO_2 Peaks Obtained in TPO Tests (Fig. 4) and Those for Desorbed Acetone in TPD Experiments (Fig. 5)

	CO_2 desorbed from TPO				Acetone from TPD	
Catalyst	Total area (a.u.)	Desorption temperature (°C)			Total area (a.u.)	Desorption temperature (°C)
MgO(II)AIR	779	155	420	522	233	347
BM50	478	482	580		55	422
MgO(I)VAC	334	408			37	295
MgO(I)AIR	—				—	—

Note. Both were carried out after 150 min reaction at 200°C.

shows the TPO profiles obtained after reactions carried out at 200°C (the monitored peak was that at $m/z = 44$, corresponding to CO_2). The area of each peak was proportional to the amount of CO_2 released and the temperature was indicative of the binding strength of carbon atoms to the catalytic sites where they formed and/or the type or carbon residue observed. The areas of CO_2 peaks and the maximum temperatures are given in Table 7. The amount of CO_2 released was correlated with the extent of deactivation of each catalyst; the most markedly deactivated solid was MgO(II)AIR, which was also that producing the most CO_2, according to the TPO profile.

The results of TPO experiments carried out after the isothermal reactions at higher temperatures suggest that the amount of CO_2 detected increased with increasing temperature, which is consistent with the fact that raising the temperature also increased deactivation. This suggests that the carbon deposit is the main, or one of the primary sources of deactivation in this type of catalyst. Additional experiments that are discussed below provided further information on the deactivation phenomenon.

TPD experiments, performed after each isothermal reaction, revealed the presence of adsorbed species on the catalyst surface which were gradually retained as the reaction progressed, thereby inactivating the anchoring sites. This, together with the carbon deposit, contributed, albeit to a lesser extent, to deactivating the catalysts.

The experiments with the magnesium oxides showed that only acetone was bound to the solid surface. Figure 5 shows the TPD profiles for acetone following the isothermal reactions at 200°C. Table 7 lists the area and maximum temperature for each peak. The catalysts with the strongest basic sites, viz. BM50 and MgO(II)AIR (20), exhibited acetone retention up to the highest temperatures tested (between 300 and 500°C), whereas those with the weakest basic sites (MgO(I)AIR and MgO(I)VAC) retained little acetone and only from 200 to 300°C. The catalyst with the highest density of basic sites, MgO(II)AIR, was also that retaining the most acetone.

The TPD results for PM2 following isothermal reaction at 200, 250, 300, and 350°C (Fig. 6) only revealed the desorption of propene. The three desorption peaks for propene at 200°C became a single one (the highest temperature peak) at 350°C.

Reaction Mechanism

The actual reaction mechanism for the conversion of 2-propanol is still incompletely elucidated; however, some of the proposed mechanisms account for both the dehydrogenation and the dehydration process (18, 26–33). It is widely accepted that the interaction between an alcohol and the surface of a metal oxide yields a mixture of adsorbed alcohol molecules and alkoxide species (31, 34).

The E1 elimination mechanism (IUPAC's designation for which is $D_N + D_H$ (35)) is a two-step pathway, the rate-determining step of which is the ionization of the substrate

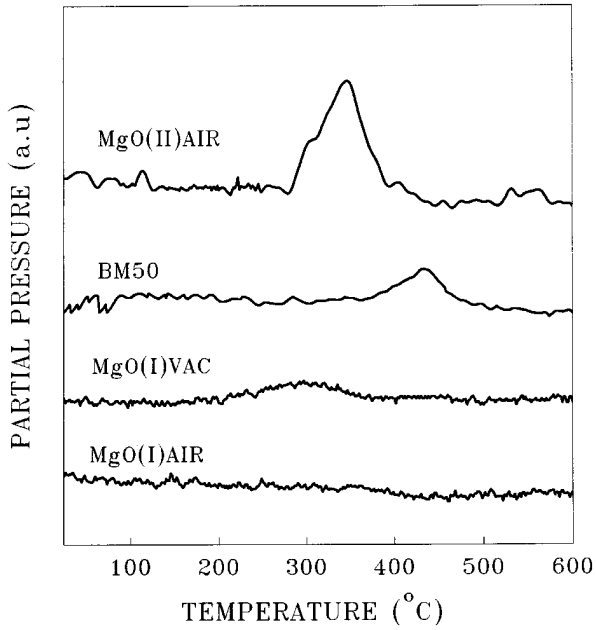

FIG. 5. TPD profiles for acetone ($m/z = 58$) obtained after isothermal decomposition (200°C for 150 min) of 2-propanol over the basic catalysts tested. Conditions: Nitrogen flow, 50 mL/min; temperature ramp, 10°C/min; catalyst weight, 50 mg.

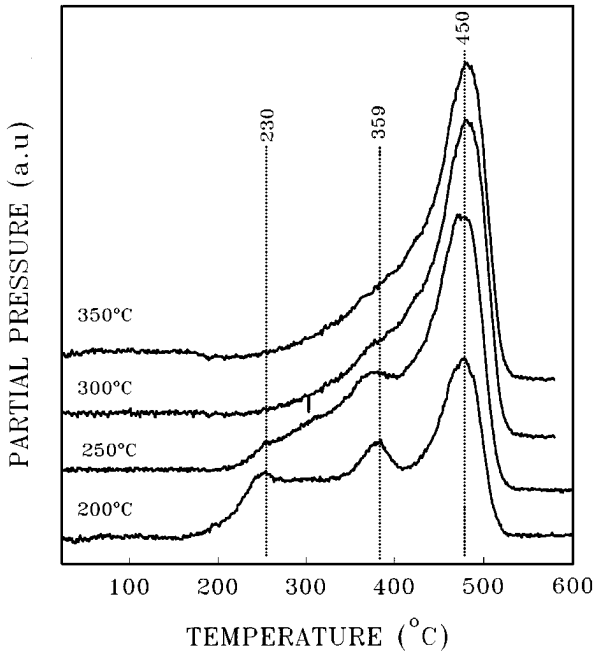

FIG. 6. TPD profiles for propene obtained after isothermal decomposition (200°C for 150 min) of 2-propanol over PM2. Conditions as in Fig. 5.

to a carbenium ion (by release of a leaving group such as OH^-) that rapidly loses a β proton. This mechanism normally operates without a base.

In the E2 mechanism (IUPAC's designation for which is $A_nD_ED_N$ (35)), both the leaving group and the proton depart simultaneously, the proton being pulled off by a base. The mechanism thus takes place in a single step.

There is a third possibility: the proton leaves first and the leaving group second. This is a two-step process called the E1cB mechanism ($A_nD_E + D_N$, according to IUPAC (35)). The intermediate is a negatively charged species (the conjugate base of the substrate). In many E1cB eliminations involving the formation of C=O bonds, the initial step (the loss of a proton) can also take place from the oxygen atom.

The three mechanisms above are more similar than different from one another. In each case there is a leaving group that departs with its electron pair and another (usually hydrogen) that comes off without it. The only difference is in the order in which they leave. It is now generally accepted that there is a spectrum of mechanisms ranging from one extreme, in which the leaving group departs well before the proton (pure E1), to the other extreme, in which the proton comes off first and then, after some time, the leaving group follows (pure E1cB). The pure E2 mechanisms would be somewhere in between, with both groups leaving simultaneously. However, most E2 reactions do not lie exactly in the middle of the two extremes.

All the proposed mechanisms rely on the same assumption: the interaction between an acid–base couple with the alcohol (29, 30, 32). Catalysts with a large number of acid sites (e.g., PM2) lead predominantly to dehydration, which takes place via an E_1 mechanism. On the other hand, dehydrogenation takes place to a limited extent only, via an E_1cB mechanism.

In solids with a large number of basic sites, both dehydrogenation and dehydration take place via an E_1cB mechanism; the former predominates over the latter. The interaction between a basic site and an alcohol molecule causes a proton to be abstracted from the alcoholic group, thus producing an adsorbed alkoxide species (Fig. 7A). The release, in a subsequent step, of a proton from the β carbon atom leads to the formation of acetone. Akiba *et al.* (27) and Yamashita *et al.* (28), using deuterated 2-propanol, found unequivocally that the formation of the acetone is preceded by the abstraction of hydrogen from the –OH group. The dehydration probably results from the interaction of a basic site with the proton of the β carbon to form an adsorbed carbanion (Fig. 7B), followed by the release of the –OH group and the consequent formation of the alkene (32).

Over solids of a similar acid–base character, the dehydration may take place via a concerted E_2 mechanism. The

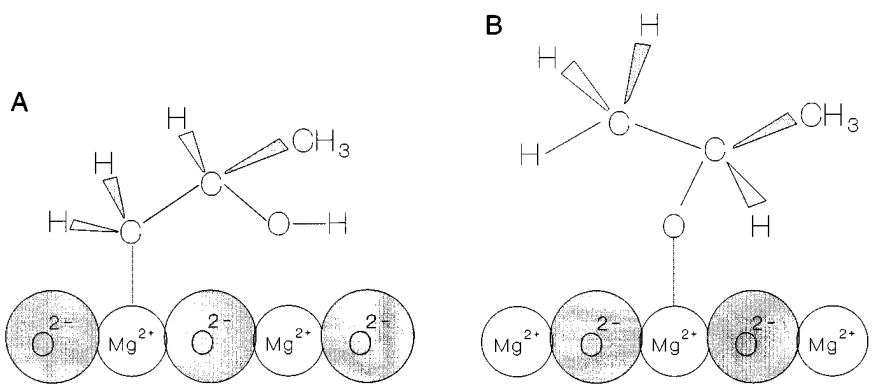

FIG. 7. Anionic species adsorbed following withdrawal of a proton from the hydroxyl group (A) or β carbon (B) according to an E1cB mechanism.

simultaneous interaction of an acid–base couple with the –OH group and the proton of the β carbon in 2-propanol would cause both groups to be released and propene to be produced.

The proposed reaction mechanism must also account for the correlations between the *pseudo*-kinetic constants and the acid–base properties shown in Table 6. The table suggests that there is a correlation between the acid properties of the solids and their *pseudo*-kinetic constants of dehydration (kK_p). Such a correlation in turn suggests an E_1 mechanism for the dehydration, where acid sites are the primary and sole actors in the process.

On the other hand, there is a good correlation between the number of basic sites and the ratio of the dehydrogenation to dehydration constant. This implies the active presence of basic sites in both processes, which suggests an E1cB mechanism that accounts for both the dehydrogenation and the dehydration and assumes the presence of basic sites that are capable of withdrawing a proton in the rate-determining step, consistent with Figs. 7A and 7B.

Finally, these proposed mechanisms are also consistent with the activation energies of dehydration and dehydrogenation obtained with the magnesium oxides and PM2 (Table 4). The fact that both parameters for the oxides of magnesium are similar is consistent with a single mechanism (E1cB) that yields both acetone and propene according to the adsorbed intermediates of Figs. 7A and 7B. On the other hand, the two activation energies for PM2 are markedly different, which suggests that the dehydration may proceed via a mechanism (E1) other than that for the dehydrogenation (E1cB). As noted earlier, elimination reactions at acid–base sites follow mechanisms that range from pure E1 to pure E1cB, with a variety of intermediate choices that depend on the strength and density of the acid and basic sites in the solids. The mid-point, where the catalyst would possess acid and basic sites of a similar strength would correspond to a concerted E2 mechanism. Also, while the dehydration may proceed via the three above-described mechanisms (E1, E1cB, or E2), the dehydrogenation can only take place via an E1cB mechanism.

CONCLUSIONS

The results obtained in this work and the above interpretation allow us to draw the following conclusions:

(a) Because of their basic character, magnesium oxides favor dehydrogenation over dehydration.

(b) The final reactivity of the oxides in the dehydrogenation of 2-propanol depends largely on the preparation method and the precursor used. Thus, *in vacuo* calcination leads to solids [MgO(I)VAC] that give much higher conversions than those synthesized by air calcination [MgO(I)AIR]. This enhanced reactivity may originate in the increased density of basic sites obtained by *in vacuo* calcination of the solids. On the other hand, the synthetic precursor used is seemingly more influential on the presence of strongly basic sites in the solids obtained from $Mg(OH)_2$, which accounts for their higher dehydrogenating activity.

(c) Doping magnesium oxide with B_2O_3 increases its dehydrating power as it increases the density of the acid (both Brønsted and Lewis) sites relative to the unaltered oxide. On the other hand, doping has little effect on the dehydrogenating activity or surface base properties.

(d) An E1cB mechanism is proposed for the decomposition of 2-propanol over magnesium oxides; the mechanism involves strong basic sites that effect the withdrawal of a proton, whether from the β carbon or the alcohol function. In this way, the mechanism yields the dehydration product (propene) via the intermediate depicted in Fig. 7B and the dehydrogenation product (acetone) via that of Fig. 7A. Alternatively, the dehydration may take place via an E1 mechanism involving strong acid sites and withdrawal of the hydroxyl group of the alcohol by the catalyst. This mechanism is consistent with the reactivity exhibited by the typically acid catalyst PM2.

(e) The catalysts are deactivated mainly by the carbon deposit formed and the adsorption of substances on their surface; as the temperature rises, adsorption of the species decreases and the amount of carbon deposited increases.

ACKNOWLEDGMENTS

The authors gratefully acknowledge funding of this research by the Consejería de Educación y Ciencia de la Junta de Andalucía and the Dirección General de Investigación Científica y Técnica (DGICyT) in the framework of Project PB92-0816. The staff at the Mass Spectrometry Service of the University of Córdoba is also acknowledged for their kind technical assistance in the experiments.

REFERENCES

1. Tanabe, K., Misono, M., Ono, Y., and Hattori, H., *in* "New Solids Acids and Bases, Their Catalytic Properties," Stud. Surf. Sci. Catal. (B. Belmon and J. T. Yates, Eds.), Vol. 51. Elsevier, Amsterdam, 1989.
2. Guisnet, M., *in* "Catalysis by Acids and Bases," Stud. Surf. Sci. Catal. (B. Imelik *et al*., Eds.), Vol. 20, p. 283. Elsevier, Amsterdam, 1985.
3. Grzybowska-Swierkosz, B., *in* "Catalysis by Acids and Bases," Stud. Surf. Sci. Catal. (B. Imelik *et al*., Eds.), Vol. 20, p. 45. Elsevier, Amsterdam, 1985.
4. Barthomeuf, D., and Figueras, F., *in* "Chemical and Physical Aspects of Catalytic Oxidation" (J. L. Portefaix and F. Figueras, Eds.), p. 241. Editions CNRS, Paris, 1980.
5. Hattori, H., Maruyama, K., and Tanabe, K., *Bull. Chem. Soc. Jpn.* **50**, 2181 (1977).
6. Hattori, H., Asada, N., and Tanabe, K., *Bull. Chem. Soc. Jpn.* **51**, 1704 (1978).
7. Tanabe, K., and Hattori, H., *Chem. Lett.* 625 (1976).
8. Fukuda, Y., Hattori, H., and Tanabe, K., *Bull. Chem. Soc. Jpn.* **51**, 3150 (1978).
9. Anderson, J. R., and Boudart, M., *in* "Catalysis, Science and Technology," Vol. 2, p. 232. Springer-Verlag, Berlin, 1982.
10. Takahashi, K., Shibagaki, M., and Matsushita, H., *Bull. Chem. Soc. Jpn.* **65**, 262 (1992).

11. Freidlin, L. K., Sharf, V. Z., German, E. N., Vorb'eva, N. K., and Shcherbakova, S. I., *Izv. Akad. Nauk USSR, Ser. Khim.* 2130 (1970).
12. Niiyama, H., and Echigoya, E., *Bull. Jpn. Pet. Inst.* **14**, 83 (1972); *Bull. Chem. Soc. Jpn.* **45**, 938 (1972).
13. Kibby, G. L., and Hall, W. K., *J. Catal.* **31**, 65 (1973).
14. Klemm, L. H., and Taylor, D. R., *J. Org. Chem.* **35**, 3216 (1970).
15. Tomczak, D. D., Allen, J. L., and Poeppelmeir, K. R., *J. Catal.* **146**, 155 (1994).
16. Krylov, O. V., "Catalysts by Non-Metals," Ch. 1. Academic Press, New York, 1970.
17. Gervasini, A., and Auroux, A., *J. Catal.* **38**, 190 (1991).
18. Waugh, K. C., Bowker, M., Petts, R. W., Vandervell, H. D., and O'Malley, *J. Appl. Catal.* **25**, 121 (1986).
19. Aramendía, M. A., Borau, V., Jiménez, C., Marinas, J. M., Porras, A., and Urbano, F. J., *Rapid Commun. Mass Spectrom.* **8**, 599 (1994).
20. Aramendía, M. A., Borau, V., Jiménez, C., Marinas, J. M., Porras, A., and Urbano, F. J., *Rapid Commun. Mass Spectrom.* **9**, 193 (1995).
21. Aramendía, M. A., Borau, V., Jiménez, C., Marinas, J. M., and Rodero, F., *Colloids Surf.* **12**, 227 (1984).
22. McKenzie, A., Fishel, C. T., and Davis, R. J., *J. Catal.* **138**, 547 (1992).
23. Beranek, L., *in* "Advances in Catalysis," Vol. 24. Academic Press, New York, 1975.
24. Ai, M., *J. Catal.* **40**, 327 (1976).
25. Beltramini, J. N., and Trimm, D. L., *React Kinet. Catal. Lett.* **37**, 313 (1988).
26. Bowker, M., Petts, R. W., and Waugh, K. C., *J. Chem. Soc. Faraday Trans. 1* **78**, 2573 (1982).
27. Akiba, E., Soma, M., Onishi, T., and Tamaru, K. Z., *Phys. Chem.* **119**, 103 (1980).
28. Yamashita, M., Dai, F-Y., Suzuki, M., and Saito, Y., *Bull. Chem. Soc. Jpn.* **64**, 628 (1991).
29. Williams, C., Makarova, M. A., Malysheva, L. V., Paukshtis, E. A., and Zamarev, K. I., *J. Chem. Soc. Faraday Trans.* **86**, 3473 (1990).
30. Grisebach, H., and Moffat, J. B., *J. Catal.* **80**, 350 (1983).
31. Hussein, G. A. M., and Sheppard, N., *J. Chem. Soc. Faraday Trans.* **85**(7), 1723 (1989).
32. Noller, H., Lercher, J. A., and Vinek, H., *Mat. Chem. Phys.* **18**, 577 (1988).
33. Kung, H. H., *in* "Transition Metal Oxides: Surface Chemistry and Catalysis," Stud. Surf. Sci. Catal. (B. Belmon and J. T. Yates, Eds.), Vol. 45. Elsevier, Amsterdam, 1989.
34. Pepe, F., and Stone, F. S., *J. Catal.* **56**, 160 (1979).
35. March, J., *in* "Advanced Organic Chemistry. Reactions, Mechanisms, and Structure," 4 ed., p. 290. Wiley, New York, 1992.